Performance of GMSK in frequency selective Rayleigh fading and multiple cochannel interferers[1]

C.Tellambura and Vijay. K. Bhargava

Department of Electrical and Computer Engineering
University of Victoria, P.O. Box 3055, MS 8610
Victoria, British Columbia
Canada V8W 3P6

Abstract - The two-ray Rayleigh fading model accounts for the frequency selective fading experienced by the received signals in some digital cellular systems. For such fading channels, binary error probabilities of GMSK with discriminator detection or differential detection are considered in the presence of multiple, Rayleigh-faded, independent, cochannel interferers. The paper drives an exact solution for the average error probability and a near-exact but less computationally intensive solution. The near-exact solution is virtually indistinguishable from the exact solution for large carrier-to-interference ratios (CIR). To establish the accuracy of the results, numerical examples are given.

I. Introduction

Gaussian minimum shift keying (GMSK) modulation is used in Global System for Mobile communications (GSM) and has been proposed for DECT (digital European cordless telephone system). As the name implies, GMSK is obtained by pre-filtering an MSK waveform with a Gaussian-shaped low-pass filter. The pre-filtering introduces a controlled amount of intersymbol interference (ISI) but in exchange reduces both the sidelobe power level and the width of the mainlobe of the power spectrum. Many authors have analyzed its performance in fading channels [1-4].

In cellular mobile radio, cochannel interference (CCI) significantly influences the achievable capacity. Thus, we study the performance of GMSK in the presence of multiple CCI signals in a frequency-selective Rayleigh fading environment. This problem, to the best of the authors' knowledge, appears to have received little attention before. To describe the problem precisely, consider an idealized hexagonal cell layout in a cellular system. Then, at a given time, for a 7-cell cluster, there could be up to six active cochannel interferers operating at the reuse distance from the point of reception. The CCI originating from the second-tier and higher-order tiers can usually be neglected. Each interferer is characterized by at least four parameters: carrier frequency offset $\delta\omega$, phase offset $\delta\phi$, bit timing offset τ, and power level σ^2. Since only CCI is considered, the interfering signals are assumed to have exactly the same frequency as the desired signal (i.e., $\delta\omega = 0$). We also ignore the constant phase offsets of the interferers, since they are cancelled out by both limiter discriminator detection (LDD) and differential detection (DD). Considering the bit timing delay, we distinguish two cases: (1) where the bit timing offset (say) τ of an interferer is random and distributed in the interval $(0, T)$ where T is the symbol duration, and (2) where $\tau = 0$. Since Case (1) is the most general and realistic, we analyze it in detail, and for comparison, we also treat Case (2). The power level of an interferer can be accommodated into the analysis by defining a CIR.

1. This research was supported by a grant from the National Sciences and Engineering Council of Canada.

II. General analysis

A. System Model

The transmitted GMSK modulated signals have the generic form

$$s_i(t) = \exp(j\phi_s(t-\tau_i, a_i)) \tag{1}$$

where $i = 0$ denotes the desired signal and $1 \le i \le L$ denote the interferers, and $\phi_s(t-\tau_i, a_i)$ is an information-bearing phase given by

$$\phi_s(t-\tau_i, a_i) = 2\pi f_d \int_{-\infty}^{t} \sum_{k=-\infty}^{\infty} a_k^i g(v-kT-\tau_i)\,dv. \tag{2}$$

The basic pulse shape is $g(t)$. In this f_d is the phase deviation constant and T is the bit duration, and τ_i is a time delay. Without loss of generality, upon setting $\tau_0 \equiv 0$, the random variable τ_i denotes a possible offset between the symbol timing epochs of the desired signal and the ith interfering signal. To make further analysis feasible, we make the following assumptions. For all the signals, the data bits a_k^i $(-\infty \le k \le \infty, 0 \le i \le L)$, which are equiprobable binary symbols from the set $\{\pm 1\}$, are assumed to be independent and identically distributed (iid). The random variables $\{\tau_i, i = 1, 2, \ldots, L\}$ are iid with each τ_i uniformly distributed in the interval $[0, T]$.

To represent the fading of the desired signal, we use the two-ray multipath model, as recommended by the Telecommunication Industry Association (TIA) standard committee [7]. This model implies that the delay-power density spectrum can be expressed as

$$G(\tau) = \sigma_s^2\delta(\tau) + \sigma_d^2\delta(\tau - \tau_d) \tag{3}$$

where σ_s^2 denotes the power of the main signal, σ_d^2 is the power of the delayed signal, and τ_d is a delay. Note that for simplicity, the interfering signals are modelled by non-selective Rayleigh fading only. Since the power of the delayed signal is considerably weaker than that of the main signal (e.g., $\sigma_s^2 \gg \sigma_d^2$), this assumption is justifiable for the interfering signals which are weaker than the desired signal in any case.

The total input to the detector can be expressed as follows:

$$e(t) = \sum_{i=-1}^{L} x_i(t) \exp(j\phi_s(t - \tau_i, a_i)) + n(t) \tag{4}$$

where $i = -1$ corresponds to the delayed component of the desired signal, $i = 0$ to the main part of the desired signal, and the remaining values to the interfering signals. This means that, in keeping with the definition in (3), $\tau_{-1} = \tau_d$ and $\tau_0 = 0$. The zero-mean, complex, wide-sense stationary, independent, Gaussian random processes $x_i(t)$ account for the Rayleigh fading experienced by the received signals and their autocorrelation functions are as follows:

$$R_{x_i}(\tau) = 0.5\overline{x_i(t)x_i^*(t-\tau)} = \sigma_i^2 J_0(2\pi f_D \tau) \tag{5}$$

where the overbar represent the average operation, $J_0(x)$ is the zero-order Bessel function of the first kind, and f_D is the maximum Doppler frequency. According to our notation and (3), we have $\sigma_{-1}^2 = \sigma_d^2$ and $\sigma_0^2 = \sigma_s^2$.

In (4), the zero-mean, complex, additive noise process $n(t)$ is also Gaussian with the autocorrelation function

$$R_n(\tau) = \sigma_n^2 \mathrm{sinc}(B_i\tau) \tag{6}$$

where $\mathrm{sinc}(x) = \sin(\pi x)/(\pi x)$. Note that since the intermediate frequency (IF) filter is assumed to be an ideal rectangular bandpass filter, the autocorrelation is the sinc function. Referring to (4), the total input to the detector can be alternatively expressed in polar notation as $e(t) = |e(t)|\exp(j\psi(t))$. Conventionally, the ratio of signal and noise powers and the ratio of signal and CCI powers determine the average probability of error. Hence, we define the following measures: signal-to-noise ratio (SNR) is defined as $\Gamma = \sigma_s^2/\sigma_n^2$, and carrier-to-interference ratio (CIR), in relation to the ith interferer, is defined as $\Lambda_i = \sigma_s^2/\sigma_i^2$, $1 \le i \le L$, and the carrier-to-delayed signal power (CDR) is $\Lambda_d = \sigma_s^2/\sigma_d^2$.

B. Exact Error Probability

Assuming ideal conditions, the output of limiter and discriminator elements is proportional to the instantaneous frequency of the input signal (i.e., the output is proportional to $\dot\psi(t)$). For DD, the phase difference between adjacent samples determines the output of the detector. Thus, given these idealizations, our a generic detector $d(t)$ is given by

$$d(t) = \begin{cases} \mathrm{Real}\left\{\dfrac{-je^*(t)\dot e(t)}{|e(t)|^2}\right\} & \text{for LDD,} \\ \mathrm{Real}\{-je(t+T/2)e^*(t-T/2)\} & \text{for DD.} \end{cases} \tag{7}$$

For the sampling instances $t = kT$, $k = 0, \pm1, \pm2, \ldots$, the sampled output of the detector may be expressed as

$$d_k = \mathrm{Real}\{-jX_kY_k^*\} \tag{8}$$

where $(X_k, Y_k) = (\dot e(kT), e(kT))$ for LDD and $(X_k, Y_k) = (e((k+1/2)T), e((k-1/2)T))$ for DD.

Without loss of generality, the error performance is evaluated based upon the d_0, which is a quadratic in two complex Gaussian variables. The estimate of a_0 is obtained as follows: $\hat a_0 = 1$ if $d_0 > 0$ and $\hat a_0 = -1$ if $d_0 < 0$. So the conditional error probability equals to $P(d_0 < 0)$ for $a_0 = 1$ and $P(d_0 > 0)$ for $a_0 = -1$. Using the results given in reference [6], the probability of error can be expressed as

$$P_e\big|_{a_0 = \pm1} = \frac{1}{2}\left\{1 \mp \frac{\mathrm{Real}(-j\rho)}{\sqrt{1 - \mathrm{Imag}^2(-j\rho)}}\right\} \tag{9}$$

where ρ is the correlation coefficient between X_0 and Y_0 given by

$$\rho = \left(\left(\overline{X_0Y_0^*}\right)\Big/\left(\overline{|X_0|^2}\,\overline{|Y_0|^2}\right)^{1/2}\right). \tag{10}$$

As will be seen shortly, ρ is a function of the binary data sequences $\{a_k^i\}$ and the bit-timing delays. Since $g(kT)$ in rapidly decreases as $|k|$ increases, it is convenient to neglect the effect of data bits a_k^i for $|k| > N$. Previous studies indicate that N can be as small as unity if $BT \ge 0.3$. Let us introduce the following notation: $\tau = \{\tau_1, \tau_2, \ldots, \tau_L\}$ and

$$\underline{a} = \{a_{-N}^0, \ldots, a_N^0, \ldots, \ldots, a_{-N}^L, \ldots, a_N^L\}. \tag{11}$$

We use the notation $P_e(\underline{a}, \tau)$ to signify the fact that P_e in (9) is in fact a function of the two variables above. To obtain the average error probability, the following two steps need to be carried out: first, integration of $P_e(\underline{a}, \tau)$ over the L-dimensional space $0 \le \tau_1 \le T, 0 \le \tau_2 \le T, \ldots, 0 \le \tau_L \le T$ yields the data-sequence dependent average error probability

$$P_e(\underline{a}) = \frac{1}{T^L}\left[\int_0^T \ldots \int_0^T P_e(\underline{a}, \tau)\, d\tau_1 d\tau_2 \ldots d\tau_L\right], \tag{12}$$

second, by noting that the data sequence vector $\underline{a}$ assume only $2^{(2N+1)(L+1)}$ distinct values, the average error probability can be expressed as

$$P_e = 2^{-(2N+1)(L+1)} \sum P_e(\underline{a}) \tag{13}$$

where the summation extends over the all possible values of the vector $\underline{a}$ in (11). To compute the exact average error probability, we must calculate a large number of L-dimensional integrals. For example, for $N = 1$ and $L = 6$, this amounts to 2^{21} of six dimensional integrals, which is computationally infeasible.

III. LIMITER DISCRIMINATOR DETECTION

In order to compute the probability of error, we simply ~~need~~ ρ in (10) ~~to be~~ evaluated for this case. By denoting $\mu_1 = |X_0|^2$ and $\mu_2 = |Y_0|^2$, and using the definitions in (8), we can readily show that

$$\rho = \left[\sum_{i=-1}^{L} \sigma_i^2 \dot{\phi}_i(t - \tau_i, a_i)\right] / \sqrt{\mu_1 \mu_2}. \tag{14}$$

Although no details are repeated here for brevity, the derivation of the joint pdf rests on the fact that if $x(t)$ is a Gaussian process, so is its derivative $\dot{x}(t)$. Moreover, the variance of the derivative is simply equal to $-d^2 R_x(t)/dt^2|_{t=0}$ where $R_x(t)$ is the autocorrelation function of the process $x(t)$.

Substituting ρ given in (14) into (9), one obtains the conditional error probability:

$$P_e(\underline{a}, \tau) = \frac{1}{2}[1 - \mathrm{sgn}(a_0)\rho]. \tag{15}$$

This can be used with equations (12) and (13) to calculate the exact average probability for this case. In the next section, an accurate approximation is introduced.

A. A Tight Approximation

Let us write the correlation coefficient ρ in (14) as

$$\rho = \rho_0 (1 + \varepsilon_1) / \sqrt{(1 + \varepsilon_2)} \tag{16}$$

Note that, according to our notaion (4), we have $\Lambda_0 = 1$. For reasonably large CIRs, we have $\Lambda_i^{-1} \ll 1$ for $1 \le i \le L$. Thus $\varepsilon_2 \ll 1$, and we get

$$\rho \approx \rho_0 (1 + \varepsilon_1 - \varepsilon_2/2). \tag{17}$$

Carrying out the averaging of this as needed in (12) and (13) over the bit-timing delays vector τ and the data sequences $\boldsymbol{a}_1, \ldots, \boldsymbol{a}_L$ gives the following:

$$P_e(\boldsymbol{a}_0) \approx \frac{1}{2}[1 - \mathrm{sgn}(a_0)\rho_0(1 - K)] \tag{18}$$

where K can be obtained by expanding the CCI terms in (14).

Since the data sequence $\boldsymbol{a}_0$ can only take 2^{2N+1} distinct values, the average error probability can then be approximated as

$$P_e \approx \frac{1}{2^{2N+1}} \sum P_e(\boldsymbol{a}_0). \tag{19}$$

where the summation extends over the all possible values of the data sequence $\boldsymbol{a}_0$. This expression, as compared to (13), needs a remarkably less computational effort and its accuracy can be observed by the numerical results presented later in this paper.

B. The effect of perfect bit alignment

To see the effect of perfect bit alignment of all interfering signals with the wanted signal, we set the $\tau = 0$ in (15). This can be used with (19) to find the average error probability.

C. The effect of CCI

To delineate the effect of CCI only, assume that both the additive thermal noise and the Doppler are negligible ($\Gamma \to \infty$ and $f_D T \to 0$), we have the probability of error given by (15) with $\rho = \rho_1$ where ρ_1 can be obtained from (14).

D. Noiselike CCI

In this paper the CCI signal is modelled as a complex Gaussian process modulated by a data signal (11). In order to simplify the ensuing calculations, the assumption that CCI is Gaussian is commonly invoked in the literature. From (4), the CCI signal is given by

$$\xi(t) = \sum_{i=1}^{L} x_i(t) \exp(j\phi_i(t - \tau_i, \boldsymbol{a}_i)). \tag{20}$$

Under the Gaussian assumption, $\xi(t)$ is simply treated as zero-mean, complex Gaussian noise with variance σ_c^2. Then the average error probability is given by (18) and with $\rho_0 = \rho_2$ where we have defined This can be used with (19) to calculate the average error probability for this case.

IV. Numerical Results

Here the error performance of GMSK is computed for a variety of cases, parameterized by the following variables: the ratio of the delay between the main and delayed components of the desired signal denoted by τ_d/T; the number of CCI sources denoted by L. In all the following calculations, unless otherwise stated, the normalized IF filter bandwidth $B_iT = 1.0$ is assumed.

A. Exact vs. Approximate

(13) and (19) are plotted in Figs. 1-2, which show the average error probability of GMSK with LDD for the cases $L = 1, 2, 3$. Similar results for GMSK with DD are depicted in Fig. 3. For brevity, the results for even larger values of L are not given here. Note that numerical integration needed in (12) consumes a prohibitive amount of computing time as the number of interferers increases. For CIR values greater than 20 dB, the exact result obtained via integration and the approximations are virtually identical. This means that the when the total CCI is very weak in comparison to the desired signal (i.e., $\Lambda \gg 1$), the error performance is not determined by the number of interferers, rather the total power of all interferers.

B. Irreducible Error Rates

The irreducible error rate of GMSK with LDD and DD as a function of the normalized Doppler (f_DT) is plotted in Fig. 4, where $\Gamma \to \infty$ and $\Lambda \to \infty$. For a given Gaussian prefilter normalized bandwidth, LDD results in a smaller error floor than that of DD. The irreducible error rate increases as the normalized Gaussian prefilter bandwidth BT decreases, a consequence of increasing ISI due to decreasing BT. These error floors occur due to the random phase modulation caused by the Doppler, and they can be substantially reduced by the use of diversity combining.

V. Conclusions

In this paper, we have analyzed the performance of GMSK with discriminator detection or differential detection in the presence of multiple, Rayleigh-faded, independent, cochannel interferers. The fading of the desired signal is modelled by the two-ray Rayleigh model, which accounts for the frequency selective fading encountered in mobile channels. An exact solution to the bit error probability that accounts for the effects of Gaussian noise, Rayleigh fading, cochannel interference, and timing delays of the cochannel interferers needs lengthy calculations. Therefore, a near-exact but less computationally intensive solution has been derived. As might be expected, when there are several weak interferers present, their combined effect can be represented by an equivalent interferer whose CIR is the reciprocal of the sum of the reciprocals of the CIRs of the individual interferers.

Acknowledgment

The authors greatly appreciate the final preparation of the manuscript by A. J. Mueller.

VI. References

[1] K. Murota and K. Hirade, "GMSK modulation for digital mobile telephony," *IEEE Trans. Commun.*, vol. COM -29, pp. 1044-1050, July 1981.

[2] S. M. Elnoubi, "Analysis of GMSK with discriminator detection in Mobile radio channels," *IEEE Trans. Veh. Technol.*, vol. VT - 35, pp. 71-76, May 1986.

[3] K. Hirade, M. Ishizuka, and F. Adachi, "Error rate performance of digital FM with discriminator detection in the presence of co-channel interference under fast Rayleigh fading environment," *Trans. Inst. Electron. Commun. Eng. Japan.*, pp. 704-709, Sept. 1978.

[4] K. Hirade, M. Ishizuka, and F. Adachi, "Error rate performance of digital FM with differential detecton in land mobile radio channel," *IEEE Trans. Veh. Technol.*, vol. VT-28, pp. 204-212, Aug. 1979.

[5] J.G. Proakis, Digital Communications, McGraw-Hill, 1989.

[6] Electronic Industries Association Specification IS-54, Dual-Mode Subscriber Equipment Compatibility Specification," EIA Project Number 2215, Dec. 1989.

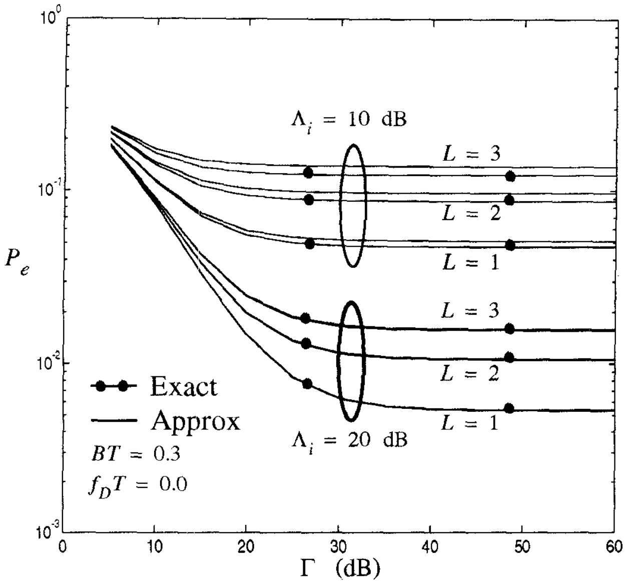

FIGURE 1. The exact and approximate bit error rates of GMSK in a Rayleigh fading environment in the presence of L cochannel interferers, The detection method is LDD. Infinite CDR is assumed.

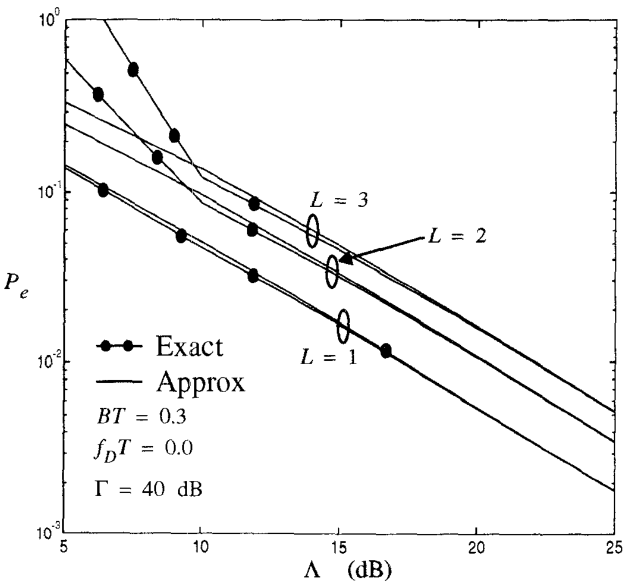

FIGURE 2. The exact and approximate bit error rates of GMSK in a Rayleigh fading environment in the presence of L cochannel interferers, The detection method is LDD. Infinite CDR is assumed.

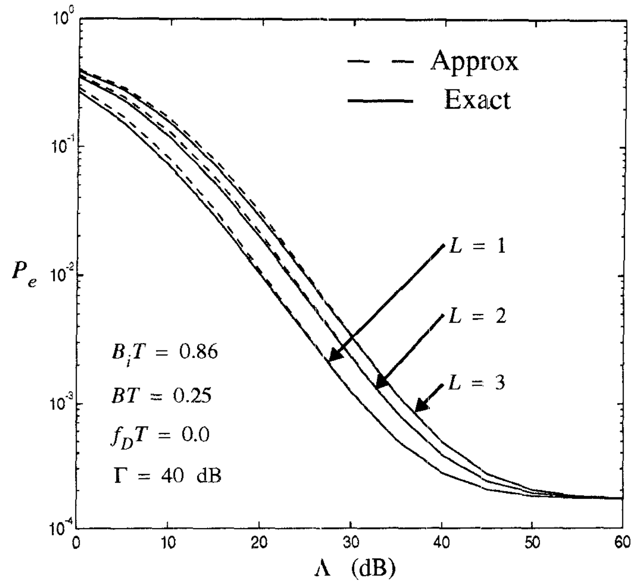

FIGURE 3. The exact and approximate bit error rates of GMSK in a Rayleigh fading environment in the presence of L cochannel interferers, The detection method is DD. Infinite CDR is assumed. The interferers have random bit-timing offsets with respect to the desired signal.

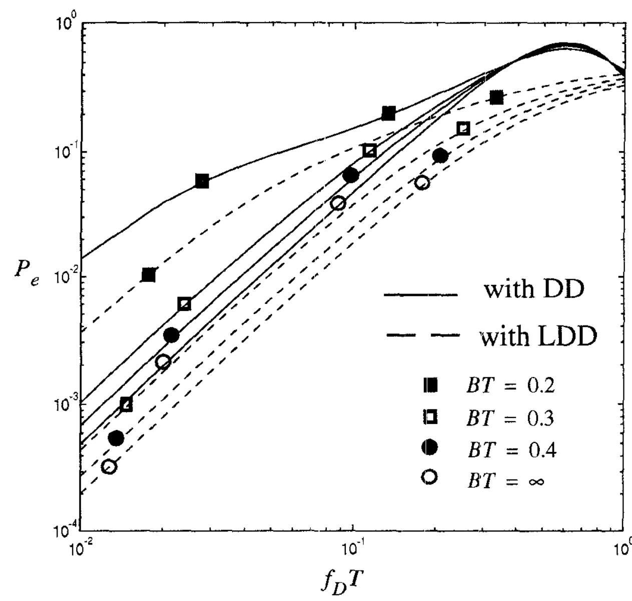

FIGURE 4. The irreducible error rate versus the normalized Doppler for GMSK in a fast Rayleigh fading channel. SNR, CDR, and CIRs are assumed to infinite.